AIAA SciTech Forum
23-27 January 2023, National Harbor, MD & Online
AIAA SCITECH 2023 Forum

10.2514/6.2023-0749

Numerical Investigation of Ignition Kernel Development with Nanosecond Pulsed Plasma in Quiescent and Flowing Mixtures

Taaresh Sanjeev Taneja*
Department of Mechanical Engineering, University of Minnesota – Twin Cities, Minneapolis, MN 55455, USA

Timothy Ombrello†
Aerospace Systems Directorate, U.S. Air Force Research Laboratory, Wright-Patterson AFB, OH 45433, USA

Joseph K. Lefkowitz ‡
Faculty of Aerospace Engineering, Technion - Israel Institute of Technology, Haifa 3200003, Israel

Suo Yang§
Department of Mechanical Engineering, University of Minnesota – Twin Cities, Minneapolis, MN 55455, USA

Nanosecond Pulsed High Frequency Discharges (NPHFD) are gaining popularity over conventional spark and arc discharges as they have been shown to increase energy efficiency, enhance ignition probability and sustained kernel growth, and offer more flexibility and control for ignition applications under various conditions. Hence, it is important to determine the impact of different factors such as the optimal pulse energy, background flow conditions, inter-pulse time, mixture equivalence ratio, etc. on the success of ignition of premixed mixtures with NPHFD. This work presents a numerical investigation of the morphology of ignition kernel development with both single-pulse and multiple-pulse discharges. Nanosecond non-equilibrium plasma discharges are modeled between pin-pin electrodes in a subsonic ignition tunnel with quiescent and flowing premixed mixtures of methane and air. Large eddy simulations (LES) are conducted to investigate the reasons for successful and failed ignition in different scenarios. A single pulse discharge in the presence of electrodes, in a quiescent medium, elucidates the gas recirculation pattern caused by the plasma pulse which results in a separated toroidal kernel from the primary ignition kernel between the electrodes. Convection heat loss to the mean flow results in quenching of the high temperature, radical-rich hot-spots creeping on the electrode walls, and leaving only the semi-toroidal kernel to propagate downstream. Finally, simulations with multiple pulses with different inter-pulse times have been conducted to analyze the synergistic effect of overlapping kernels with high temperature and OH concentration, which has been attributed as the primary reason for higher ignition probabilities in the "fully coupled" regime reported in the experiments. Successful ignition kernel formation is reported with 3 pulses at a pulse repetition frequency of 300 kHz in the fully coupled regime. This kernel volume was almost 4 times, and develops in two-thirds the time, compared to the ignition kernel volume formed by the single pulse discharge with the same total energy. Ten pulses with twice as much total energy were deposited at a much lower frequency of 2 kHz, which resulted in disjoint hot-spots that fail to form an ignition kernel in the decoupled regime.

I. Nomenclature

u_i	=	i^{th} velocity component
e	=	total internal energy per unit mass
e_{vib}	=	vibrational energy per unit mas
h_s	=	sensible enthalpy per unit mass

*Ph.D. Candidate, Student Member AIAA.
†Senior Research Aerospace Engineer, Associate Fellow AIAA.
‡Assistant Professor, Member AIAA.
§Richard & Barbara Nelson Assistant Professor, suo-yang@umn.edu (Corresponding Author), Senior Member AIAA.

e_s = sensible internal energy per unit mass
H = total non-chemical enthalpy per unit mass
E = total non-chemical energy per unit mass
p = gas pressure
T = gas temperature
t = time
ρ = gas density
τ_{ij} = viscous stress tensor
σ_{ij} = total stress tensor
D_{N_2} = diffusion coefficient of N_2
e_{sk} = sensible energy of species k
$\Delta h^o_{f,k}$ = formation enthalpy of species k
Y_k = mass fraction of species k
$V_{k,i}$ = i^{th} component of the mixture-averaged diffusion velocity of species k
$\dot{\omega}^c_k$ = net molar production rate of species k due to combustion
Q_{reac} = heat release rate due to combustion reactions
C_v = specific heat at constant volume
R_u = universal gas constant
σ_{pulse} = input energy density
r = radial coordinate in the discharge zone
τ_{pulse} = plasma pulse duration
η = fraction of total deposited power used for dissociating O_2
α = fraction of total deposited power towards vibrational energy production
e^{eq}_{vib} = equilibrium vibrational energy per unit mass
τ_{VT} = time-scale of vibrational-to-translational relaxation
Y_{O_2} = instantaneous mass fraction of oxygen
$Y^f_{O_2}$ = mass fraction of oxygen in fresh mixture
Re_τ = Turbulent Reynolds number

II. Introduction

Nanosecond non-equilibrium plasma assisted combustion (PAC) has gained popularity due to its relatively lower input power requirements, fast gas heating, the possibility of leveraging non-equilibrium plasma chemistry at low temperatures [1] and the ease of non-equilibrium plasma igniter integration within practical combustors to promote faster ignition, reduce emissions as well as ensure flame stability at harsh operating conditions (e.g., in ultra-lean combustion, and in scramjets). Hence, it is important to determine the ideal operating conditions such as pulse duration, energy density per pulse, inter-pulse time, distance between electrodes, applied voltage, etc. for practical non-equilibrium plasma based igniters used in such applications. Lefkowitz and Ombrello [2] presented a parametric exploration of the dynamics of ignition using nanosecond pulsed high frequency discharges (NPHFD) in flowing mixtures of methane and air. Three different regimes were observed based on the pulse repetition frequency (PRF) - fully coupled, partially coupled and decoupled. Ignition probabilities were calculated by performing experiments with varying number of pulses and PRFs for each regime. The fully-coupled regime occurs for the highest PRF (lowest inter-pulse time) and shows maximum ignition probability. The partially-coupled regime occurs for intermediate PRFs (intermediate inter-pulse time) and shows the lowest ignition probabilities. The decoupled regime occurs for the lowest PRFs (highest inter-pulse time) and exhibits multiple non-interacting kernels with ignition probabilities being a linear function of the number of pulses. While the outcomes of the decoupled and fully-coupled regimes are in line with intuition, the lowest ignition probability observed for the partially-coupled regime seems to be anomalous. Thus, it is of primary interest to probe into the ignition dynamics of the partially-coupled regime and determine the physical reasons governing the hypothesized "destructive coupling" of multiple interacting ignition kernels, potentially resulting in lowest ignition probabilities for this regime. In order to probe into this, modeling the discharge physics during a single plasma pulse, and the hydrodynamics and thermo-chemistry after the discharge accurately is very important. The dependency on the effect of previous pulses gets reduced for the decoupled regime, given the longer time duration between two pulses, which essentially creates fresh-gas like mixtures for every pulse and is characterized by ample space for the evolution of each ignition kernel independent of the previous one. Hence, in the present work, emphasis is laid on both aspects -

modeling the individual discharges as accurately as possible, with computational feasibility as an important constraint, and also on modeling multiple pulses and the inter-pulse time between them in a domain representative of the subsonic ignition tunnel used to perform experiments in Lefkowitz and Ombrello [2]. More recently, Mao et al. [3] numerically investigated the effect of frequency, number of pulses and flow velocity on the critical ignition volume and minimum ignition energy for plasma assisted H_2-air ignition in a 2D axisymmetric configuration of a needle-ring electrode setup. They showed that the minimum ignition energy rises with increasing flow velocity for a single pulse discharge due to increase in convection heat loss and flame stretch. Moreover, they reported ignition success with a two-pulse train only for very high frequencies, i.e., in the fully coupled regime, and attributed it to the overlap of OH radicals and due to the higher reduced electric fields, given the lower number densities of the burnt gases very close to the inter-electrode gap. Lefkowitz et al. [4] also reported high OH radical accumulation at higher pulse repetition frequencies (> 10 kHz) for CH_4-air mixtures using OH-PLIF and schlieren imaging.

Different approaches have been adopted by researchers for modeling of PAC, from detailed modeling of coupled plasma and combustion kinetics in 0D constant pressure / volume reactors [5, 6] and 1D parallel plate reactors [7], to streamer kinetics and dynamics modeling with varied levels of assumptions such as lumped vibrational energy and local field approximation, to reduce cost in 2D [8–10] to resolving "isothermal" streamers in 3D and coupling low temperature plasma solvers with low Mach combustion solvers to solve for multi-pulse discharges [11] in different types of electrode configurations.

In this work, we present simulations of NPHFD in flowing mixtures of methane and air at two different equivalence ratios and discuss the effect of total deposited plasma energy, frequency of pulsing and convection heat loss by the flowing premixed fuel-air mixture on the success of ignition kernel formation and sustenance. Ignition kernel formation due to a single pulse discharge in a quiescent medium is compared with a single pulse discharge in a flowing medium. Next, the effect of frequency and equivalence ratio is investigated by other simulations in the fully coupled and decoupled regimes, by dividing the total energy into three and ten pulses, respectively. Detailed modeling of plasma assisted combustion achieved using pin-pin discharges, in 3 dimensions for a long physical duration is a computationally expensive task. Especially while accounting for turbulent flows in large domains, with relatively high cell counts. Thus, a phenomenological plasma model proposed in Castela et al. [12] has been used, which aims to only model the most important effects of a plasma discharge such as ultra-fast dissociation of species, ultra-fast gas heating and the ultra-fast increase of vibrational energy density and the slower mode of gas heating via vibrational-to-translational relaxation. This model achieves this approximately, without solving for the detailed plasma kinetics and dynamics of streamer formation which significantly reduces the computational overhead.

III. Numerical Methodology

The phenomenological model proposed by Castela et al. [12] has been coupled with a reacting pressure-based solver implemented in-house [13, 14] within OpenFOAM [15]. The detailed list of governing equations, plasma closure modeling and the numerical treatment used while solving for the pressure and sensible enthalpy, both during and after the discharge has been provided in Taneja and Yang [14]. The equations are listed here to maintain completeness, albeit without discussion to maintain brevity.

$$\frac{\partial(\rho u_j)}{\partial t} + \frac{\partial(\rho u_i u_j)}{\partial x_i} = -\frac{\partial p}{\partial x_j} + \frac{\partial \tau_{ij}}{\partial x_i} \tag{1}$$

$$\frac{\partial(\rho Y_k)}{\partial t} + \frac{\partial(\rho u_i Y_k)}{\partial x_i} = -\frac{\partial}{\partial x_i}\left(\rho V_{k,i} Y_k\right) + W_k \dot{\omega}_k^c + W_k \dot{\omega}_k^p \tag{2}$$

$$\frac{\partial(\rho H)}{\partial t} + \frac{\partial(\rho u_i H)}{\partial x_i} = -\frac{\partial q_i}{\partial x_i} + \frac{\partial(\tau_{ij} u_i)}{\partial x_i} + \frac{\partial p}{\partial t} - \frac{\partial}{\partial x_i}\left(\rho \sum_{k=1}^{N_{sp}} h_{s,k} Y_k V_{k,i}\right) + \dot{Q}_{reac} + \dot{E}_{heat}^p + \dot{R}_{VT}^p \tag{3}$$

$$H = h_s + \frac{1}{2} u_i u_i \tag{4}$$

$$\frac{\partial(\rho e_{vib})}{\partial t} + \frac{\partial(\rho u_i e_{vib})}{\partial x_i} = -\frac{\partial}{\partial x_j}\left(\rho D \frac{\partial e_{vib}}{\partial x_i}\right) + \dot{E}_{vib}^p - \dot{R}_{VT}^p \tag{5}$$

$$\dot{E}^p = \frac{\sigma_{pulse}}{\tau_{pulse}} erfc\left(\frac{r^2}{a}\right)^b \tag{6}$$

$$\begin{aligned} \dot{\omega}^p_O &= \eta \frac{Y_{O_2}}{Y^f_{O_2}} \frac{\dot{E}^p}{e_O} \\ \dot{\omega}^p_{O_2} &= -\frac{W_O}{W_{O_2}} \dot{\omega}^p_O \end{aligned} \tag{7}$$

$$\dot{E}^p_{chem} = \frac{\eta Y_{O_2}}{Y^f_{O_2}} \left(1 - \frac{W_O e_{O_2}}{W_{O_2} e_O}\right) \dot{E}^p \tag{8}$$

$$\dot{E}^p_{heat} = \alpha \dot{E}^p - \dot{E}^p_{chem} \tag{9}$$

$$\dot{E}^p_{vib} = (1 - \alpha) \dot{E}^p \tag{10}$$

$$\dot{R}^p_{VT} = \frac{\rho(e_{vib} - e^{eq}_{vib}(T))}{\tau_{VT}} \tag{11}$$

$$e^{eq}_{vib}(T) = \frac{\frac{R_u}{W_{N_2}} \Theta_1}{e^{\Theta_1/T} - 1} \tag{12}$$

$$\tau_{VT} = \left(\frac{1}{\tau^O_{VT}} + \frac{1}{\tau^{O_2}_{VT}} + \frac{1}{\tau^{N_2}_{VT}}\right)^{-1} \tag{13}$$

Similar to Castela et al. [12], the power density is assumed to remain constant with time during the pulse and the model constants, a and b in Eq. 6, are adjusted based on the discharge gap of 2 mm such that the total deposited energy matches a desired input value. In these first sets of simulations, the energy fractions for ultra-fast dissociation of O_2, ultra-fast gas heating and ultra-fast vibrational energy increase are chosen to be 0.35, 0.20 and 0.45, respectively. In this work, a slightly smaller version of a subsonic ignition tunnel domain has been modeled with cross-sectional dimensions of 30 mm $\times$ 30 mm and a length of 120 mm. The actual experimental cross-sectional dimensions are 38.1 mm $\times$ 38.1 mm as mentioned in Lefkowitz and Ombrello [2], however, using a smaller domain ensures fewer grid points and obviates the resolution or modeling of the flow near the walls. Two pin electrodes with a gap distance of 2 mm are located 15 mm downstream of the inlet of the tunnel. The mesh is refined from the domain boundaries to the inter-electrode gap, with the smallest cell size of 16 μm in the inter-electrode gap region. The mesh comprises of approximately 17 million hexahedral-dominant elements. *snappyHexMesh* is used to perform this successive refinement and create inflation layers at the walls of the electrodes. Subsonic inlet boundary conditions are used at the inlet face and non-reflecting (waveTransmissive BC in OpenFOAM) boundary conditions are used at all other faces of the domain to avoid any numerical reflection of acoustic waves off the boundaries. Non-reflecting boundary conditions are used at all faces for the quiescent flow simulations discussed in Section IV. A zero-gradient boundary condition for pressure, temperature (i.e. adiabatic) and mass fractions of all species, and a no-slip boundary condition for velocity is imposed at the electrode walls. More accurate temperature and species mass fraction BCs, to capture the effect of the loss of heat and radicals to the walls, will be used in future work. The time step was fixed at 0.5 ns during the plasma discharge and was calculated dynamically based on a maximum CFL number of 0.5 for all simulations after the discharge. It ranged from 0.5 ns to 5 μs after the discharge. Second order, total variation diminishing central difference schemes were used for the gradient, divergence and laplacian terms of all the governing equations. Implicit time integration is done with a first order Euler scheme. Moreover, RANS with the k-ω SST model was used to obtain a statistically stationary initial velocity profile and pressure distribution for the turbulent flow in the ignition tunnel. The coarse mesh RANS results were mapped onto the finer LES mesh for all the cases with flow.

A 30-species reduced GRI-Mech 3.0 mechanism [16] has been used to perform all the simulations. To ensure accurate estimation of thermodynamic quantities at temperatures as high as 5000 K in some of the simulations, the NASA-7 polynomial coefficients from Goos et al.'s [17] database were used.

Large eddy simulations (LES) using the dynamic Smagorinsky model for the sub-grid Reynolds stresses and the Partially Stirred Reactor Model for the sub-grid chemical source terms have been performed in this work. Verification of the solver using 2D simulations was done with Castela et al. [12], followed by comparison of DNS and LES results in quiescent and isotropic turbulent environments for the 3D cube results which were compared to results in Castela et al. [18].

IV. Results and Analysis

A. Effect of Background Mean Flow

The verification of the solver for the quiescent and isotropic turbulent cases in 2D was provided in [14]. Two single-pulse discharge simulations with equal energy deposition of 15 mJ and $\phi = 0.9$ (CH_4-air) are performed here with and without mean flow. As is discussed in Castela et al. [18], a shock wave emanates from the center of the domain and propagates outward by losing energy and eventually gets converted to a weak acoustic wave, that exits the domain with non-reflecting outlets. Moreover, consistent with the observations of Dumitrache et al. [19] and Castela et al. [18], for high enough deposited energies, the initial cylindrical shaped kernel collapses into a toroidal shaped kernel. The associated recirculation of the mixture after the discharge creates almost fresh gas like conditions if the inter-pulse time between two subsequent pulses is long enough. The quiescent case serves as a benchmark to assess the role of the mean flow on the ignition kernel morphology development in the other simulation. As can be seen from Fig. 1, the ignition kernel splits into a toroidal kernel which keeps getting pushed away from the electrodes and other connected lobes creep up along the surfaces of the electrodes and keep expanding. At around 1.8 ms, the toroidal lobe and the electrode-bound lobe expand significantly enough to re-join to eventually form a larger and sustained ignition kernel. However, as can be seen in Fig. 1, the convection heat loss to the mean flow (with uniform inlet velocity of 10 m/s) and flame stretch result in the quenching of the lobes attached to the electrode walls. Thus, only the semi-toroidal lobe formed after the splitting of the ignition kernel keeps propagating downstream in the ignition tunnel. The combustion heat release overcomes the shear and diffusion due to the mean flow and the kernel is observed to keep growing, thus confirming successful ignition. However, the primary ignition kernel in the quiescent case grows much faster and larger in volume around 1.5 ms itself. On the other hand, the growth of the ignition kernel with the mean flow supposedly takes much longer than 3 ms to occupy a comparable volume. The difference in size and morphology of the ignition kernels for these two single-pulse discharge cases can qualitatively be seen in Fig. 2 which shows the gradients of mass density (i.e., numerical Schlieren). Quantitative estimations of the ignition kernel growth rate and volume will be done in future, as a function of mean flow velocity and pulse energy. It must again be noted that these simulations do not account for any heat or radical loss to the electrode walls, and thus they show rather optimistic scenarios as compared to the experiments.

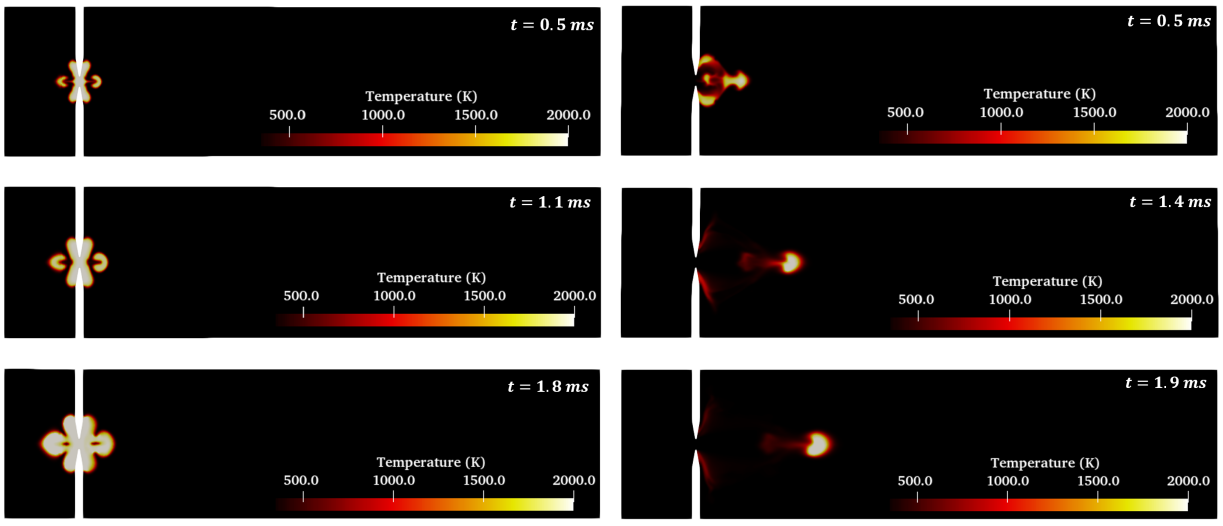

Fig. 1 Temperature Evolution in quiescent (left) and flowing (right) mixtures of CH_4-air.

Fig. 2 Gradient of mass density (Numerical Schlieren) in quiescent (left at 1.8 ms) and flowing (right at 2.4 ms) mixtures of CH_4-air.

B. Effect of Pulse Frequency and Rate of Energy Deposition

In this subsection, two simulations were performed with different pulse repetition frequencies, spanning the fully coupled and decoupled regimes described in Lefkowitz and Ombrello [2]. The frequencies for the fully coupled and decoupled cases are 300 kHz and 2 kHz respectively. Total energy of 15 mJ was divided into 3 pulses, each depositing 5 mJ for the fully coupled case. This value was chosen to be equal to the baseline single pulse discharge cases discussed in the previous subsection. Whereas, a total of 34 mJ was deposited in the decoupled case with 10 pulses each depositing 3.4 mJ. It should also be noted that the equivalence ratios for the fully coupled and decoupled cases was 0.9 and 0.6, respectively, at the time of submission of this manuscript. Another simulation with the higher equivalence ratio will be done in the decoupled regime as well, to ensure better comparative analysis. Nevertheless, key features regarding the synergy of pulses resulting in the kernel shape evolution can still be individually assessed with the results presented here.

Two consecutive pulses are deposited 0.5 ms apart (i.e., at a frequency of 2 kHz) in the decoupled case. Thus, the background gas convects by approximately 5 mm between two pulses (mean velocity of 10 m/s). The approximate stream-wise diameter of the radical-rich, high temperature kernel produced by a single pulse, with 3.4 mJ of total energy, is about 2.5 - 3 mm, as can be estimated from Fig. 3. Thus, every successive pulse “sees" an almost fresh gas like mixture. Both the temperature and OH mass fraction contours in Fig. 3 show this lack of synergy between pulses, which ultimately leads to failure of ignition kernel formation. The 10 individual pulses, which add more than twice as much energy as the fully coupled case, only locally heat the gas but do not form an interacting kernel. This can be seen from the numerical schlieren plot in Fig. 5.

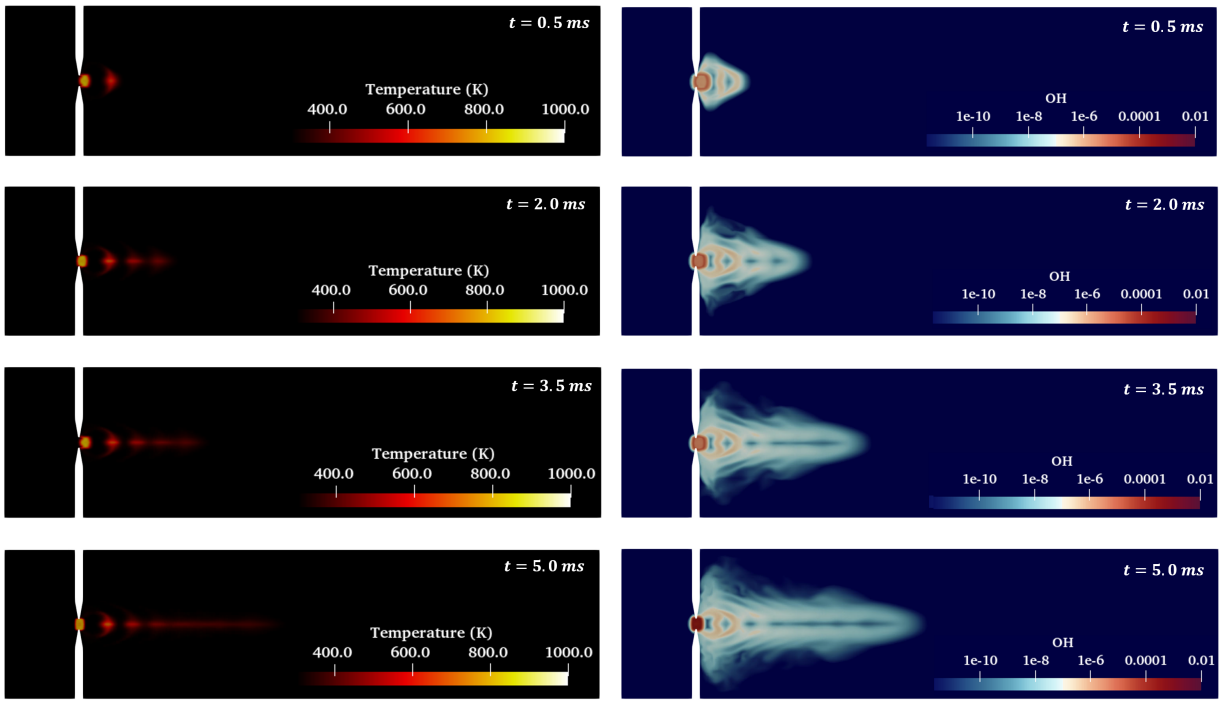

Fig. 3 Temperature and OH mass fraction evolution - Decoupled Case (PRF - 2 KHz).

The fully coupled case with a frequency of 300 kHz resulted in a large sustained ignition kernel in a much shorter amount of time. Compared to the ignition kernel produced by the single pulse discharge with the same amount of total energy of 15 mJ, at 2.4 ms, the kernel produced by the three pulses which are deposited only 3.33×10^{-6} s apart from each other, is almost 4 times larger in volume (comprised of iso-surfaces of temperatures above 1300 K). This can mainly be attributed to the overlap of high-temperature and radical-rich kernels produced by the 3 successive pulses, which can be seen in Fig. 4. Moreover, this kernel develops in 1.6 ms, which is much faster than the sustained kernel formation by the single pulse discharge. The peculiar jet-like, stretched structure of the expanding ignition kernel (Fig. 5) can be attributed to the accelerated flow in the center of the domain due to the constriction created by the electrode separation. The low-speed recirculation region created by the bluff bodies (electrodes) forms a shear layer with the accelerating flow that crosses the electrode gap, and then decelerates as the flow spreads outwards. The local velocity immediately downstream of the electrode gap ranges from 13 - 18 m/s (for a mean inlet velocity of 10 m/s) after the strong compression wave dissipates substantially. Thus, the central core of the ignition kernel keeps getting accelerated forward, thereby enhancing the jet-like structure of the kernel. This also causes the primary ignition kernel to separate from the lobes attached to the electrode walls. The resolution downstream is not very fine, and thus the vortical structures of the kernel that are seen in the experiments of Lefkowitz and Ombrello [2] are not observed in this LES study.

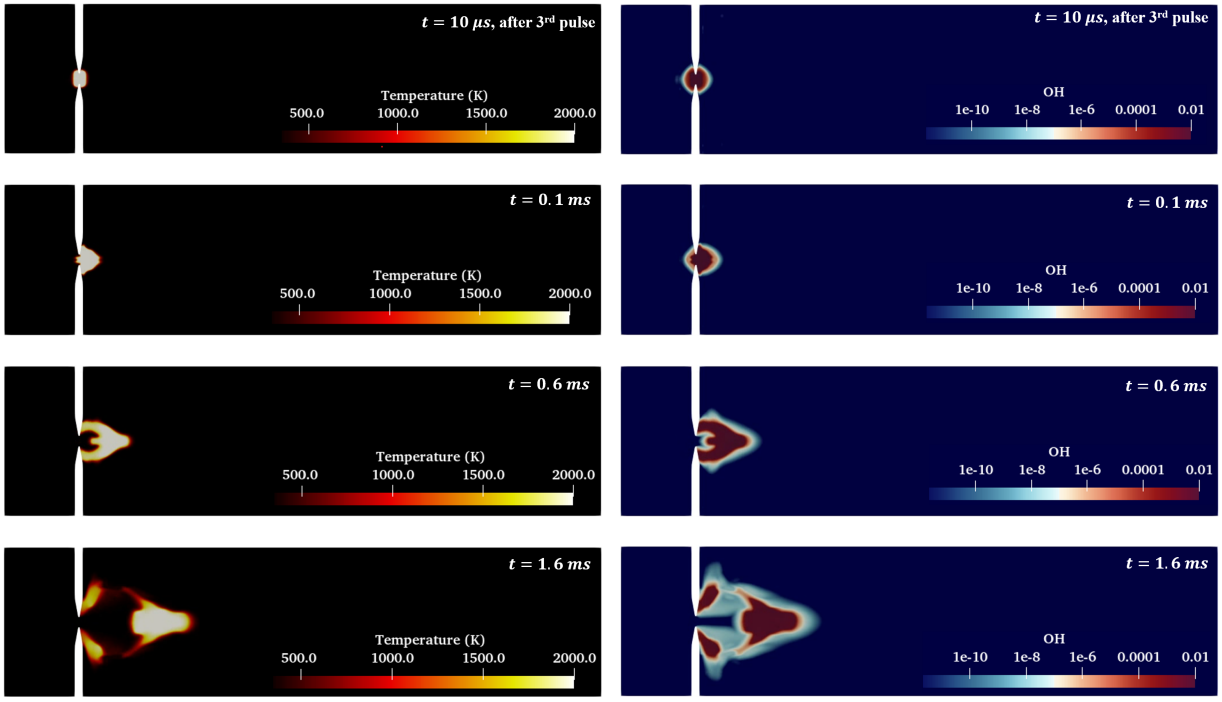

Fig. 4 Temperature and OH mass fraction evolution - Fully Coupled Case (PRF - 300 KHz).

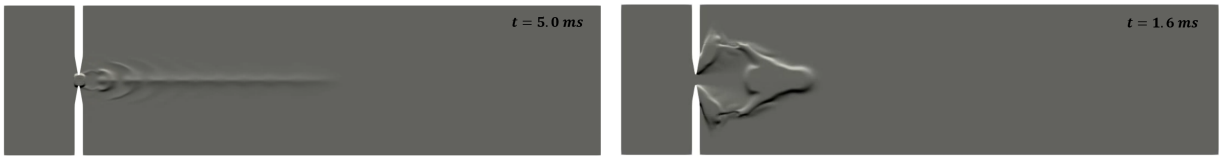

(a) Failed Ignition in the Decoupled Regime

(b) Successful Ignition in the Fully Coupled Regime

Fig. 5 Gradient of mass density for fully coupled case (300 kHz, 3 pulses, 5 mJ per pulse) (left, at 1.6 ms) and decoupled case (2 kHz, 10 pulses, 3.4 mJ per pulse) (right, at 5.0 ms).

V. Conclusion and Future Work

A phenomenological model that obviates the direct simulation of the detailed plasma kinetics and streamer dynamics has been used to numerically investigate the ignition kernel development using nanosecond pulsed high frequency discharges (NPHFD) in quiescent and flowing mixtures of CH_4-air. The effect of mean flow, pulse energy deposition, and pulse repetition frequency on the success of a sustained ignition kernel formation has been studied. It was found that the high-temperature, radical-rich hot kernel first splits into two lobes, a toroidal lobe which gets pushed away from the central core and another lobe that expands along the walls of the two pin electrodes. These lobes keep expanding in a quiescent environment and eventually re-join to form a large ignition kernel. However, mean flow causes flame stretch and local quenching of the electrode-bound lobes. Consequently, the semi-toroidal lobe keeps propagating downstream and expanding to form a ignition kernel that is much smaller. Moreover, the synergistic effect of OH accumulation and overlap of high temperature hot-spots created by 3 pulses in the fully coupled regime lead to a much larger and faster growing ignition kernel. On the contrary, the decoupled case features 10 individual pulses which only locally heat the gas without constructively interacting to form a sustainable ignition kernel, despite adding more than twice the total energy.

At the time of submission of this manuscript, a simulation in the partially coupled regime with 3 pulses, each depositing 5 mJ of energy, at a PRF of 5 kHz has not progressed sufficiently to comment on the success or failure of ignition. This will be reported and discussed in future. Quantitative estimations for minimum ignition energy and minimum kernel volume will also be conducted.

Acknowledgments

S. Yang acknowledges the grant support from NSF CBET 2002635. T.S. Taneja acknowledges the support from the UMII MnDRIVE Graduate Assistantship Award. The authors also acknowledge the Minnesota Supercomputing Institute (MSI) and Prof. Graham V. Candler for the computational resources.

References

[1] Ju, Y., Lefkowitz, J. K., Reuter, C. B., Won, S. H., Yang, X., Yang, S., Sun, W., Jiang, Z., and Chen, Q., "Plasma assisted low temperature combustion," *Plasma Chemistry and Plasma Processing*, Vol. 36, No. 1, 2016, pp. 85–105.

[2] Lefkowitz, J. K., and Ombrello, T., "An exploration of inter-pulse coupling in nanosecond pulsed high frequency discharge ignition," *Combustion and Flame*, Vol. 180, 2017, pp. 136–147.

[3] Mao, X., Zhong, H., Wang, Z., Ombrello, T., and Ju, Y., "Effects of inter-pulse coupling on nanosecond pulsed high frequency discharge ignition in a flowing mixture," *Proceedings of the Combustion Institute*, 2022.

[4] Lefkowitz, J. K., Hammack, S. D., Carter, C. D., and Ombrello, T. M., "Elevated OH production from NPHFD and its effect on ignition," *Proceedings of the Combustion Institute*, Vol. 38, No. 4, 2021, pp. 6671–6678.

[5] Taneja, T. S., Johnson, P. N., and Yang, S., "Nanosecond pulsed plasma assisted combustion of ammonia-air mixtures: Effects on ignition delays and NOx emission," *Combustion and Flame*, Vol. 245, 2022, p. 112327.

[6] Lefkowitz, J. K., Guo, P., Rousso, A., and Ju, Y., "Species and temperature measurements of methane oxidation in a nanosecond repetitively pulsed discharge," *Philosophical Transactions of the Royal Society A: Mathematical, Physical and Engineering Sciences*, Vol. 373, No. 2048, 2015, p. 20140333.

[7] Yang, S., Nagaraja, S., Sun, W., and Yang, V., "Multiscale modeling and general theory of non-equilibrium plasma-assisted ignition and combustion," *Journal of Physics D: Applied Physics*, Vol. 50, No. 43, 2017, p. 433001.

[8] Barleon, N., Cheng, L., Cuenot, B., Vermorel, O., and Bourdon, A., "Investigation of the impact of NRP discharge frequency on the ignition of a lean methane-air mixture using fully coupled plasma-combustion numerical simulations," *Proceedings of the Combustion Institute*, 2022.

[9] Tholin, F., and Bourdon, A., "Simulation of the hydrodynamic expansion following a nanosecond pulsed spark discharge in air at atmospheric pressure," *J. Phys. D. Appl. Phys.*, Vol. 46, 2013, p. 365205.

[10] Mao, X., Zhong, H., Zhang, T., Starikovskiy, A., and Ju, Y., "Modeling of the effects of non-equilibrium excitation and electrode geometry on H2/air ignition in a nanosecond plasma discharge," *Combustion and Flame*, Vol. 240, 2022, p. 112046.

[11] Sitaraman, H., and Grout, R., "Premixed combustion simulations with a self-consistent plasma model for initiation," *54th AIAA Aerospace Sciences Meeting*, 2016, p. 2158.

[12] Castela, M., Fiorina, B., Coussement, A., Gicquel, O., Darabiha, N., and Laux, C. O., "Modelling the impact of non-equilibrium discharges on reactive mixtures for simulations of plasma-assisted ignition in turbulent flows," *Combustion and flame*, Vol. 166, 2016, pp. 133–147.

[13] Zhou, D., Zhang, H., and Yang, S., "A Robust Reacting Flow Solver with Computational Diagnostics Based on OpenFOAM and Cantera," *Aerospace*, Vol. 9, No. 2, 2022, p. 102.

[14] Taneja, T. S., and Yang, S., "Comparing Low-Mach and Fully-Compressible CFD Solvers for Phenomenological Modeling of Nanosecond Pulsed Plasma Discharges with and without Turbulence," *AIAA SCITECH 2022 Forum*, 2022, p. 0976.

[15] Jasak, H., "OpenFOAM: open source CFD in research and industry," *International Journal of Naval Architecture and Ocean Engineering*, Vol. 1, No. 2, 2009, pp. 89–94.

[16] Lu, T., and Law, C. K., "A criterion based on computational singular perturbation for the identification of quasi steady state species: A reduced mechanism for methane oxidation with NO chemistry," *Combustion and Flame*, Vol. 154, No. 4, 2008, pp. 761–774.

[17] Goos, E., Burcat, A., and Ruscic, B., "Extended third millennium ideal gas and condensed phase thermochemical database for combustion with updates from active thermochemical tables," *Elke Goos, Remchingen, Germany, accessed Sept*, Vol. 19, 2010, p. 2016.

[18] Castela, M., Stepanyan, S., Fiorina, B., Coussement, A., Gicquel, O., Darabiha, N., and Laux, C. O., "A 3-D DNS and experimental study of the effect of the recirculating flow pattern inside a reactive kernel produced by nanosecond plasma discharges in a methane-air mixture," *Proceedings of the Combustion Institute*, Vol. 36, No. 3, 2017, pp. 4095–4103.

[19] Dumitrache, C., Gallant, A., Minesi, N., Stepanyan, S., Stancu, G. D., and Laux, C. O., "Hydrodynamic regimes induced by nanosecond pulsed discharges in air: mechanism of vorticity generation," *Journal of Physics D: Applied Physics*, Vol. 52, No. 36, 2019, p. 364001.